



I S A V

**Journal of Theoretical and Applied
Vibration and Acoustics**

journal homepage: <http://tava.isav.ir>



Primary resonance of an Euler-Bernoulli nano-beam modelled with second strain gradient

Hossein Mohammadi ^{*a}, Soroush Sepehri ^b

^aAssistant Professor, School of Mechanical Engineering, Shiraz University, Shiraz, Islamic Republic of Iran

^bPhd. student, School of Mechanical Engineering, Tehran University, Tehran, Islamic Republic of Iran

ARTICLE INFO

Article history:

Received 15 March 2019

Received in revised form
25 May 2019

Accepted 5 June 2019

Available online 10 June 2019

Keywords:

Second strain gradient theory,

Nonlinear vibration,

Euler-Bernoulli beam,

Method of multiple scales.

ABSTRACT

In the present manuscript, the second strain gradient (SSG) is utilized to investigate the primary resonance of a nonlinear Euler-Bernoulli nanobeam is analyzed in this paper for the first time. To that end, the second strain gradient theory, a higher-order continuum theory capable of taking the size effects into account, is utilized and the governing equation of the motion for an Euler-Bernoulli nanobeam is derived with sixteen higher-order material constants. Then by implementing the Galerkin's method, the Duffing equation for the vibration of a hinged-hinged nanobeam is obtained and its primary resonance is studied utilizing the method of multiple scales. The size effects and impact of various system parameters on the amplitude of the response are then investigated for three different materials and the results are compared to that of the first strain gradient and classical theories. The results of this manuscript clearly shows that the nonlinear vibration of a second strain gradient nanobeam is size-dependent and although the difference between the results obtained by the second strain gradient theory and the first strain gradient theory is negligible for thicker beams, as the thickness decreases, the difference becomes more prominent. Also, the effects of nonlinearity on the forced vibration nonlinear response of an SSG beam are investigated and some observations are reported.

© 2019 Iranian Society of Acoustics and Vibration, All rights reserved.

1. Introduction

Nowadays, the growing interest in using micro- and nano-electromechanical systems (MEMS and NEMS) such as shock sensors [1] micro-actuators [2], bio-MEMS [3] and so on have made them interesting fields of research and hence, scholars have shown great interest in modeling

* Corresponding author.

E-mail addresses: h_mohammadi@shirazu.ac.ir (H. Mohammadi)
<http://dx.doi.org/10.22064/tava.2019.106342.1135>

static and dynamic behaviors of different elements of such structures. When the dimensions of a beam reduces to the sub-micron level, size-dependent behavior will arise [4] and the classical theories become incapable of taking the size-dependency of such small-scale structures into account. Therefore, the need for a non-classical theory capable of doing so arises and hence, various higher-order continuum theories such as the higher-order gradient theories and couple stress theory have been proposed to consider higher-order stresses in addition to the classical stress and predict the size-dependent mechanical behavior of small-scale structures in which, aside from the classical material parameters, there may exist some higher-order length-scale parameters in the corresponding constitutive relation.

Couple stress theory which was proposed by Koiter and Mindlin in the 1960s [5, 6], introduces two higher-order material parameters in addition to the Lamé constants in the constitutive equations. The definition of these constants makes the couple stress theory suitable for predicting the size-dependent behaviors. Su and Liu [7] used the couple stress theory and proposed an effective dynamic continuum model to investigate the behavior of free vibrations of periodic cellular solids.

In 2002, the modified couple stress theory with only one higher-order material constant was proposed by Yang *et al.*[8]. Based on this theory, he developed a linear elastic model for isotropic materials. Using the Modified couple stress, Park and Gao[9] presented a new model for the bending of an Euler-Bernoulli beam model using the minimum total potential energy principle. Later, a nonlinear Timoshenko beam model based on the modified couple stress theory was developed by Asghari *et al.*[10]. Furthermore, the modified couple stress modelling of functionally graded Euler-Bernoulli and Timoshenko beams was developed by Asghari *et al.* [11, 12].

In 1965, a more general form of the strain gradient theory, namely, the second strain gradient theory (SSG) was proposed by Mindlin[13]. In doing so, he introduced sixteen higher-order material constants assuming the potential energy-density to be a function of the first and second derivatives of the strain tensor. Using this theory, a geometrically nonlinear Euler-Bernoulli beam model was presented by Karparvarfard *et al.*[14]. In a more recent article, the second strain gradient theory was used by Momeni and Asghari to develop a size-dependent formulation for the functionally graded micro/nanobeams[15]. Furthermore, in 2012, the analytical formulation of the sixteen material constants associated with the second strain gradient theory corresponding to fcc metals was given in terms of the parameters of Sutton-Chen interatomic potential function by Shodja *et al.*[16].

In 1968, the (first) strain gradient theory was proposed by Mindlin [17] as a special case of the strain gradient theory in which the strain energy-density was taken to be only the function of the first derivative of the strain tensor. This reduced the number of higher-order material constants in the corresponding constitutive equations from sixteen to five. Ansari *et al.* [18] incorporated this theory, as the most general strain gradient elasticity theory, into classical Timoshenko beam theory and developed a size-dependent beam model to investigate the static and dynamic behavior of functionally graded nanobeams.

Another version of the strain gradient theory with three higher-order material constants was suggested by Lam *et al.* [19] based on which, Asghari *et al.* [20] developed a nonlinear size-dependent Euler-Bernoulli beam model. In another article, Mohammadi and Mahzoon [21] presented a model for postbuckling of Euler-Bernoulli microbeams and showed that small-scale

parameters have a significant influence on the postbuckling behavior of microbeams. Furthermore, strain gradient theory was used by Mohammadi and Sepehri [22] to investigate the bifurcation behavior of an Euler Bernoulli micro/nanobeam.

In comparison to the first strain gradient, much fewer attempts have been made to predict mechanical behavior of a system using the second strain gradient theory and although some researchers have used this theory to present the Euler-Bernoulli [23] and Timoshenko [15] beam models, a report on the nonlinear vibration characteristics of a nanobeam modelled by the SSG theory is yet to be made. Hence, in this paper, the nonlinear primary resonance of a hinged second strain gradient Euler-Bernoulli nanobeam made of three distinct materials is investigated and the effects of various system parameters such as the excitation amplitude on the vibrational behavior of the system are illustrated. Further, it is found that there is a critical value for the frequency of the system after which the vibration of the SSG micro/nanobeam becomes multivalued.

2. Governing Equation

According to the second strain gradient theory presented by Mindlin[13], the strain energy density U_0 is a function of three-polyadic:

$$U_0 = U_0(\varepsilon_1, \varepsilon_2, \varepsilon_3). \tag{1}$$

in which, ε_1 is the classical infinitesimal strain with six independent components and ε_2 and ε_3 are the strain gradient and second strain gradient tensors, respectively. Taking ∇ and \mathbf{u} to be the gradient operator and the displacement vector, one may write:

$$\begin{aligned} \varepsilon_{ij} &= \frac{1}{2} [\nabla \mathbf{u} + (\nabla \mathbf{u})^T]_{ij} = \frac{1}{2} (u_{i,j} + u_{j,i}), \\ \eta_{ijk} &= [\nabla \nabla \mathbf{u}]_{ijk} = \frac{\partial^2 u_k}{\partial x_i \partial x_j}, \\ \xi_{ijkl} &= [\nabla \nabla \nabla \mathbf{u}]_{ijkl} = \frac{\partial^3 u_l}{\partial x_i \partial x_j \partial x_k}. \end{aligned} \tag{2}$$

in the previous equations, the components of the displacement vector \mathbf{u} are denoted by u_i , while the components of the infinitesimal strain tensor $\boldsymbol{\varepsilon}$, the first strain gradient tensor $\boldsymbol{\eta}$ and the second strain gradient tensor $\boldsymbol{\xi}$ are designated by $\varepsilon_{ij}, \xi_{ijkl}$ and ξ_{ijkl} , respectively.

Using the aforementioned definitions, the strain energy density for a linear isotropic centrosymmetric material can be written as:

$$\begin{aligned} U_0 &= \frac{1}{2} \lambda \varepsilon_{ii} \varepsilon_{jj} + \mu \varepsilon_{ij} \varepsilon_{ij} + a_1 \eta_{ijj} \eta_{ikk} + a_2 \eta_{iik} \eta_{kjj} + a_3 \eta_{iik} \eta_{jjk} + a_4 \eta_{ijk} \eta_{ijk} + a_5 \eta_{ijk} \eta_{kji} \\ &\quad + b_1 \xi_{iijj} \xi_{kkll} + b_2 \xi_{ijkk} \xi_{ijll} + b_3 \xi_{iijk} \xi_{jjkl} + b_4 \xi_{iijk} \xi_{llkj} + b_5 \xi_{iijk} \xi_{iijk} \\ &\quad + b_6 \xi_{ijkl} \xi_{ijkl} + b_7 \xi_{ijkl} \xi_{jkli} + c_1 \varepsilon_{ii} \xi_{jjkk} + c_2 \varepsilon_{ij} \xi_{ijkk} + c_3 \varepsilon_{ij} \xi_{kkij} + b_0 \xi_{iijj}, \end{aligned} \tag{3}$$

In eq (3), The two quadratic products of the classical infinitesimal tensor (ε_1) are denoted by λ and μ , which are the well-known Lamé constants. Besides, higher-order material constants a_1 to

a_5 are the constant coefficients of the quadratic products of the strain gradient (ε_2) components. Furthermore, length-scale parameters b_1 to b_7 are the coefficients of seven products of the second strain gradient components (ε_3) and c_1 to c_3 are the coefficients of the product of ε_1 components with ε_3 . The remaining length-scale parameter (b_0) is a modulus of cohesion presented by Mindlin[13]. It should be noted that the second strain gradient is responsible for the surface tension, while the coupling terms c_1 to c_3 are responsible for the free surface effects [24]. Also, it is important to know that the five coefficients a_1 to a_5 have dimension of force and are also present in Toupin's strain gradient theory [25], while the coefficients b_1 to b_7 and c_1 to c_3 are of the dimensions of force times squared length and force, respectively and b_0 has the dimension of force.

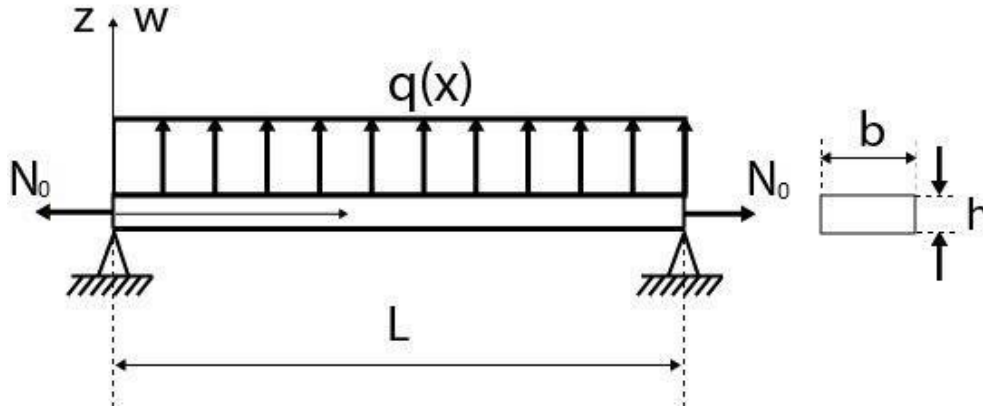


Fig 1. An Euler-Bernoulli hinged-hinged beam with height h , width b and uniform rectangular cross section.

An Euler-Bernoulli hinged beam with uniform rectangular cross section, height h and width, subjected to a distributed load $q(x)$ and axial load N_0 , is shown in Figure 1. For such a beam, based on the Euler-Bernoulli beam theory, the components of the displacement field can be described as:

$$u_1 = u(x, t) - z \frac{\partial w(x, t)}{\partial x}, u_2 = 0, u_3 = w(x, t), \quad (4)$$

Combining (2) with (4) the nonzero components of tensors are obtained as below:

$$\begin{aligned} \varepsilon_{11} &= \frac{\partial u}{\partial x} - z \frac{\partial^2 w}{\partial x^2}, \\ \eta_{111} &= \frac{\partial \varepsilon_{11}}{\partial x}, \eta_{311} = \frac{\partial \varepsilon_{11}}{\partial z}, \eta_{131} = -\eta_{113} = -\frac{\partial^2 w}{\partial x^2}, \\ \xi_{1111} &= \frac{\partial^2 \varepsilon_{11}}{\partial x^2}, \xi_{3111} = \xi_{1311} = \frac{\partial^2 \varepsilon_{11}}{\partial x \partial z}, \xi_{1131} = \xi_{1113} = -\frac{\partial^3 w}{\partial x^3}. \end{aligned} \quad (5)$$

Implementing the von Karman assumption, one may write:

$$\varepsilon_{11} = \frac{\partial u}{\partial x} - z \frac{\partial^2 w}{\partial x^2} + \frac{1}{2} \left(\frac{\partial w}{\partial x} \right)^2. \quad (6)$$

In (6) the term $\frac{1}{2} \left(\frac{\partial w}{\partial x} \right)^2$ accounts for the mid-plane stretching.

Then, after writing the expressions for the strain energy (U), the kinetic energy (T) and the work done by external forces (W), Hamilton's principle can be utilized to derive the governing equations for the motion of the nanobeam.

$$\int_{t_1}^{t_2} (\delta T - \delta U + \delta W) dt = 0 \tag{7}$$

Applying Hamilton's principle, the equation of motion of the second strain gradient nonlinear Euler-Bernoulli beam is obtained:

$$\begin{aligned} & \frac{\partial}{\partial x} \left[N_0 + EA \left(\frac{\partial u}{\partial x} + \frac{1}{2} \left(\frac{\partial w}{\partial x} \right)^2 \right) \right. \\ & - 2A(a_1 + a_2 + a_3 + a_4 + a_5 - c_1 - c_2 - c_3) \frac{\partial^2}{\partial x^2} \left(\frac{\partial u}{\partial x} + \frac{1}{2} \left(\frac{\partial w}{\partial x} \right)^2 \right) \\ & \left. + 2A(b_1 + b_2 + b_3 + b_4 + b_5 + b_6 + b_7) \frac{\partial^4}{\partial x^4} \left(\frac{\partial u}{\partial x} + \frac{1}{2} \left(\frac{\partial w}{\partial x} \right)^2 \right) \right] = \rho A \frac{\partial^2 u}{\partial t^2}, \end{aligned} \tag{8}$$

$$\begin{aligned} & - \frac{\partial}{\partial x} \left\{ \left[N_0 + EA \left(\frac{\partial u}{\partial x} + \frac{1}{2} \left(\frac{\partial w}{\partial x} \right)^2 \right) \right. \right. \\ & - 2A(a_1 + a_2 + a_3 + a_4 + a_5 - c_1 - c_2 - c_3) \frac{\partial^2}{\partial x^2} \left(\frac{\partial u}{\partial x} + \frac{1}{2} \left(\frac{\partial w}{\partial x} \right)^2 \right) \\ & \left. + 2A(b_1 + b_2 + b_3 + b_4 + b_5 + b_6 + b_7) \frac{\partial^4}{\partial x^4} \left(\frac{\partial u}{\partial x} + \frac{1}{2} \left(\frac{\partial w}{\partial x} \right)^2 \right) \right] \frac{\partial w}{\partial x} \right\} + k_1 \frac{\partial^4 w}{\partial x^4} \\ & - (k_2 - 2k_3) \frac{\partial^6 w}{\partial x^6} + k_4 \frac{\partial^8 w}{\partial x^8} + \rho A \frac{\partial^2 w}{\partial t^2} - \rho I \frac{\partial^4 w}{\partial x^2 \partial t^2} + c \frac{\partial w}{\partial t} = q(x, t) \end{aligned}$$

Where

$$\begin{aligned} k_1 &= EI + 2A(a_1 - a_2 + a_3 + 3a_4 - a_5), \\ k_2 &= 2I(a_1 + a_2 + a_3 + a_4 + a_5) + 2A(2b_2 - 2b_4 + 2b_5 + 4b_6), \\ k_3 &= I(c_1 + c_2 + c_3), \\ k_4 &= 2I(b_1 + b_2 + b_3 + b_4 + b_5 + b_6 + b_7). \end{aligned} \tag{9}$$

and $\rho, I = \int_A z^2 dA$ and A are density, the moment of inertia about y-axis and area, respectively.

The term $c \frac{\partial w}{\partial t}$ is the force exerted on the system by a viscous damper with the damping coefficient C .

Also, within the framework of the second strain gradient theory, the boundary conditions can be defined as below. It is worth mentioning that for the end-section of the beam, only one of the two types of boundary conditions, namely essential (geometric) and natural (loading) can be imposed.

$$\begin{aligned} & \left[N_0 + EA \left(\frac{\partial u}{\partial x} + \frac{1}{2} \left(\frac{\partial w}{\partial x} \right)^2 \right) - 2A(a_1 + a_2 + a_3 + a_4 + a_5 - c_1 - c_2 - c_3) \frac{\partial^2}{\partial x^2} \left(\frac{\partial u}{\partial x} + \frac{1}{2} \left(\frac{\partial w}{\partial x} \right)^2 \right) \right. \\ & \left. + 2A(b_1 + b_2 + b_3 + b_4 + b_5 + b_6 + b_7) \frac{\partial^4}{\partial x^4} \left(\frac{\partial u}{\partial x} + \frac{1}{2} \left(\frac{\partial w}{\partial x} \right)^2 \right) - \bar{N} \right]_{x=0,L} = 0 \text{ or } \delta u|_{x=0,L} = 0, \end{aligned} \tag{10}$$

$$\left[A(2a_1 + 2a_2 + 2a_3 + 2a_4 + 2a_5 - c_1 - c_2 - c_3) \frac{\partial}{\partial x} \left(\frac{\partial u}{\partial x} + \frac{1}{2} \left(\frac{\partial w}{\partial x} \right)^2 \right) - 2A(b_1 + b_2 + b_3 + b_4 + b_5 + b_6 + b_7) \frac{\partial^3}{\partial x^3} \left(\frac{\partial u}{\partial x} + \frac{1}{2} \left(\frac{\partial w}{\partial x} \right)^2 \right) - \bar{P} \right] \quad (11)$$

$$= 0 \text{ or } \delta \left(\frac{\partial u}{\partial x} + \frac{1}{2} \left(\frac{\partial w}{\partial x} \right)^2 \right) = 0,$$

$$\left[2A(b_1 + b_2 + b_3 + b_4 + b_5 + b_6 + b_7) \frac{\partial^2}{\partial x^2} \left(\frac{\partial u}{\partial x} + \frac{1}{2} \left(\frac{\partial w}{\partial x} \right)^2 \right) + A(c_1 + c_2 + c_3) \left(\frac{\partial u}{\partial x} + \frac{1}{2} \left(\frac{\partial w}{\partial x} \right)^2 \right) + Ab_0 - \bar{R} \right] \quad (12)$$

$$= 0 \text{ or } \delta \left(\frac{\partial}{\partial x} \left(\frac{\partial u}{\partial x} + \frac{1}{2} \left(\frac{\partial w}{\partial x} \right)^2 \right) \right) = 0,$$

$$\left\{ \left[N_0 + EA \left(\frac{\partial u}{\partial x} + \frac{1}{2} \left(\frac{\partial w}{\partial x} \right)^2 \right) - 2A(a_1 + a_2 + a_3 + a_4 + a_5 - c_1 - c_2 - c_3) \frac{\partial^2}{\partial x^2} \left(\frac{\partial u}{\partial x} + \frac{1}{2} \left(\frac{\partial w}{\partial x} \right)^2 \right) + 2A(b_1 + b_2 + b_3 + b_4 + b_5 + b_6 + b_7) \frac{\partial^4}{\partial x^4} \left(\frac{\partial u}{\partial x} + \frac{1}{2} \left(\frac{\partial w}{\partial x} \right)^2 \right) \right] \frac{\partial w}{\partial x} \right\} \quad (13)$$

$$- k_1 \frac{\partial^4 w}{\partial x^4} + (k_2 - 2k_3) \frac{\partial^5 w}{\partial x^5} - k_4 \frac{\partial^7 w}{\partial x^7} + \rho I \frac{\partial^4 w}{\partial x^2 \partial t^2} - \bar{V} = 0 \text{ or } \delta w = 0,$$

$$k_1 \frac{\partial^2 w}{\partial x^2} - (k_2 - 2k_3) \frac{\partial^4 w}{\partial x^4} + k_4 \frac{\partial^6 w}{\partial x^6} - \bar{M} = 0 \text{ or } \delta \left(\frac{\partial w}{\partial x} \right) = 0, \quad (14)$$

$$(k_2 - k_3) \frac{\partial^3 w}{\partial x^3} - k_4 \frac{\partial^5 w}{\partial x^5} - \bar{Q} = 0 \text{ or } \delta \left(\frac{\partial^2 w}{\partial x^2} \right) = 0, \quad (15)$$

$$k_4 \frac{\partial^4 w}{\partial x^4} + k_3 \frac{\partial^2 w}{\partial x^2} - \bar{K} = 0 \text{ or } \delta \left(\frac{\partial^3 w}{\partial x^3} \right) = 0. \quad (16)$$

Note that in the preceding equations \bar{N} and \bar{V} are the classical axial and shear resultants, respectively and \bar{M} is the resultant moment acting on the end section. \bar{P} , \bar{Q} , \bar{R} , and \bar{K} are the resultants of higher-order stress components. As can be seen in Eqs.(10)-(16), the SSG theory suggests that higher-order boundary conditions can pose a restriction on the second and third variations of the deflections as well as the deflection and slope. On the contrary, the classical theories only restrain the deflection and the slope of the ends, while the first strain gradient theory imposes constraints on the second variation of the deflection as well, but neglects the third variation.

1.1 A Hinged-Hinged Beam

For a beam with hinged-hinged boundary conditions, one may write:

$$u(0, t) = u(l, t) = 0, \quad (17)$$

$$w(0, t) = w(l, t) = 0, \quad (18)$$

It should also be noted that in a hinged-hinged beam, the support does not resist against any strain, strain gradient, rotation or curvature. As a consequence, one may assume all the resultants

of the classical and higher-order stress components to be zero, i.e $\bar{N} = \bar{V} = \bar{P} = \bar{Q} = \bar{R} = \bar{K} = 0$. In other words, the work conjugates to $\frac{\partial u}{\partial x} + \frac{1}{2} \left(\frac{\partial w}{\partial x}\right)^2$, $\frac{\partial}{\partial x} \left(\frac{\partial u}{\partial x} + \frac{1}{2} \left(\frac{\partial w}{\partial x}\right)^2\right)$, $\frac{\partial w}{\partial x}$, $\frac{\partial^2 w}{\partial x^2}$, and $\frac{\partial^3 w}{\partial x^3}$ are neglected and accordingly, equations (11), (12), (14), (15) and (16) are easily satisfied.

Now, by implementing (17) and (18) in (10)-(16) and performing some mathematical manipulations, the following eighth-order differential equation can be obtained:

$$k_1 \frac{\partial^4 w}{\partial x^4} - (k_2 - 2k_3) \frac{\partial^6 w}{\partial x^6} + k_4 \frac{\partial^8 w}{\partial x^8} - N \frac{\partial^2 w}{\partial x^2} + \rho A \frac{\partial^2 w}{\partial t^2} + c \frac{\partial w}{\partial t} = q(x, t), \tag{19}$$

in which

$$N = N_0 + \frac{EA}{2l} \int_0^l \left(\frac{\partial w}{\partial x}\right)^2 dx. \tag{20}$$

To have a parametric study of the mechanical and vibrational behavior of the SSG nanobeam, a normalization of the governing equations and the boundary conditions is necessary. To that end, the following nondimensional parameters are defined:

$$X = \frac{x}{l}, \quad W = \frac{w}{l}, \quad \tau = \kappa^2 \sqrt{\frac{EI}{\rho Al^4}} t. \tag{21}$$

where κ is a constant that depends on the boundary conditions. The values of κ for hinged-hinged and clamped-clamped boundary conditions are reported to be π and 4.73 respectively[26].

By substituting the normalized parameters in the governing equation, Eq. (19) can be described in nondimensional form as:

$$K_1 \frac{\partial^4 W}{\partial X^4} - (K_2 - 2K_3) \frac{\partial^6 W}{\partial X^6} + K_4 \frac{\partial^8 W}{\partial X^8} - \tilde{N} \frac{\partial^2 W}{\partial X^2} + \frac{\partial^2 W}{\partial \tau^2} + c \frac{\partial W}{\partial \tau} = \tilde{Q}(X, \tau), \tag{22}$$

in which the following parameters are described for simplicity:

$$\begin{aligned} K_1 &= \frac{1 + \frac{24}{Eh^2}(a_1 - a_2 + a_3 + 3a_4 - a_5)}{\pi^4}, \\ K_2 &= \frac{\left(\frac{2}{E}\right)(a_1 + a_2 + a_3 + a_4 + a_5) + \frac{24}{Eh^2}(2b_2 - 2b_4 + 2b_5 + 4b_6)}{l^2 \pi^4}, \\ K_3 &= \frac{(c_1 + c_2 + c_3)}{El^2 \pi^4}, \\ K_4 &= \frac{2(b_1 + b_2 + b_3 + b_4 + b_5 + b_6 + b_7)}{El^4 \pi^4}, \\ \tilde{N} &= \tilde{N}_0 + \frac{6}{\pi^4} \left(\frac{l}{h}\right)^2 \int_0^l \left(\frac{\partial W}{\partial X}\right)^2 dX, \\ \tilde{N}_0 &= \frac{N_0 l^2}{\pi^4 EI}, \\ \tilde{Q}(X, \tau) &= \frac{ql^3}{\pi^4 EI}. \end{aligned} \tag{23}$$

3. Primary Resonance

With the aim of investigating the primary resonance of a second strain gradient nanobeam, Galerkin's Method will be utilized to transfer the governing equations into time-domain. After multiplying both sides of Eq.(22) by the corresponding mode shape and integrating from 0 to 1, the nonlinear duffing equation is reached. Note that for a hinged-hinged nanobeam, the mode shape is $W(X, \tau) = W(\tau) \sin \pi X$. For the case of primary resonance, the initial axial load is taken to be zero, i.e. $N_0 = 0$. Further, to investigate the forced vibration, the external harmonic force is taken to be of the form $\hat{Q} = \varepsilon^2 K_Q \sin(\Omega\tau)$. Hence, the governing equation can be written as:

$$\dot{W} + \beta^2 W + \varepsilon \alpha W^3 = -2\varepsilon \eta \dot{W} + \varepsilon K_Q \sin(\Omega\tau), \tag{24}$$

Where

$$\begin{aligned} \beta^2 &= K_1 \pi^4 + (K_2 - 2K_3) \pi^6 + K_4 \pi^8 \\ \varepsilon \alpha &= \frac{3l^2}{h^2}, \end{aligned} \tag{25}$$

Now by implementing the multiple-scale method [27] the following system of linear equations based on different powers of ε can be obtained:

$$O(\varepsilon^0): D_0^2 W_0 + \beta^2 W_0 = 0, \tag{26}$$

$$O(\varepsilon^1): D_0^2 W_1 + \beta^2 W_1 = -2D_0 D_1 W_0, \tag{27}$$

$$(\varepsilon^2): D_0^2 W_2 + \beta^2 W_2 = -2D_0 D_1 W_1 - 2D_0 D_2 W_0 - D_1^2 W_0 - \eta D_0 W_0 - \alpha W_0^3 + K_Q \sin(\Omega\tau), \tag{28}$$

The general solution of the W_0 can be written as:

$$W_0 = A(T_1) \exp(i\beta T_0) + \bar{A}(T_1) \exp(-i\beta T_0), \tag{29}$$

where \bar{A} is the complex conjugate of A.

Now, by substituting W_0 from(29) in (27), it is found that any particular solution of (27) has a secular term containing the factor $\pm \exp(i\beta T_0)$ unless:

$$D_1 A = 0. \tag{30}$$

Elimination of the secular terms in(28) gives:

$$i\eta A \beta + 3\alpha A^2 \bar{A} + 2i\beta A' = 0. \tag{31}$$

In order to eliminate the secular terms in (31), A is written in polar form as below:

$$A = \frac{1}{2} a \exp(i\theta). \tag{32}$$

Substituting (32) in(31) and separating the real and imaginary parts, the set

$$a' = -\eta a + \frac{1}{2} \frac{K_Q}{\beta} \sin \theta, \tag{33}$$

$$a\theta' = \sigma a - \frac{3}{8} \frac{\alpha}{\beta} a^3 + \frac{1}{2} \frac{K_Q}{\beta} \cos \gamma \tag{34}$$

Now by considering the steady-state condition for the motion, $a' = \theta' = 0$, the system of equations for the system takes the form of:

$$\eta a = \frac{1}{2} \frac{K_Q}{\beta} \sin \theta, \tag{35}$$

$$\sigma a - \frac{3}{8} \frac{\alpha}{\beta} a^3 = -\frac{1}{2} \frac{K_Q}{\beta} \cos \theta. \tag{36}$$

By squaring and adding (35) and (36), the frequency response equation is obtained as:

$$\left(\eta^2 + \left(\sigma - \frac{3}{8} \frac{\alpha}{\beta^2} \right)^2 \right) \cdot a^2 = \frac{K_Q^2}{4\beta^2}. \tag{37}$$

In order to get numeric results, the dimensions of the micro/nanobeam are taken to be $= 0.6a_T$, $l = 30b$, and $h = 0.6b$. Furthermore, the nanobeam is assumed to be made of three distinct materials of aluminum, nickel, and gold, for which the Young Modulus and material length scale parameters are listed in Table 1 and Table 2 [16]:

Table 1. Young modulus and higher-order material constants a_i 's for Al, Ni, and Au [28]

	E (GPa)	a_T (Å)	a_1 (eV/Å)	a_2 (eV/Å)	a_3 (eV/Å)	a_4 (eV/Å)	a_5 (eV/Å)
Al	68.9	4.04	0.1407	0.0027	-0.0083	0.0966	0.2584
Ni	200	3.52	0.2386	0.0134	0.0013	0.0934	0.2462
Au	78	4.08	0.2994	0.0944	0.0944	0.0458	0.0312

Table 2. Higher-order material parameters b_i 's and c_i 's for Al, Ni and Au [28]

	b_1	b_2	b_3	b_4	b_5	b_6	b_7	c_1	c_2	c_3
Al	0.7927	0.0644	-0.1943	-0.0009	-0.0009	16.1566	48.5291	0.5041	0.3569	0.1782
Ni	0.8185	0.0821	-0.2552	-0.0020	-0.0020	15.6264	46.9584	1.1567	0.7849	0.4744
Au	0.1614	-0.0021	-0.0145	-0.0002	-0.0002	0.8134	2.4440	0.9941	0.5259	0.4413

The frequency-response curve of a nonlinear second strain gradient (SSG) Euler-Bernoulli nanobeam is depicted in Figure 2. The size-dependency of the nonlinear forced vibration of a second strain gradient nanobeam is clearly visible from Figure 2, i.e. although the length-to-thickness and width-to-the thickness ratio are kept constant, a change in the thickness also changes the amplitude of the response. It is also interpreted that by decreasing the aforementioned ratio, one can reduce the deviation of the nonlinear system from the linear state and hence the hardening nonlinearity of the nanobeam. The same deduction was carried out by [28] for a (first) strain gradient Euler-Bernoulli micro/nanobeam.

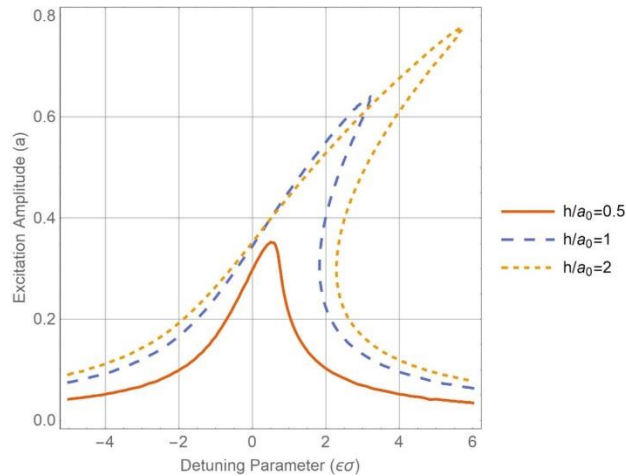


Fig 2. The frequency-response curve of a nonlinear SSG Euler-Bernoulli nanobeam for different values of h/a_0

The effect of the excitation amplitude on the frequency response curve of a primary resonance second strain gradient nanobeam is depicted in Figure3. It is obvious that a higher excitation amplitude leads to higher peak amplitude in a nanobeam in primary resonance. It is also observed that the amplitude of excitation does not change the deviation from the linear state and hence it does not affect the nonlinearity of the system. Figure3 also clearly illustrates that a nonlinear vibrating system can have up to three answers of which two are stable and one is unstable. These stable and unstable solutions lead to the jump phenomenon which is one of the most prominent characteristics of a nonlinear system. The effect of the excitation amplitude on the jump height of the Aluminum nanobeam is also shown in Figure3. It is concluded that a system may attain higher jump heights by increasing the excitation amplitude.

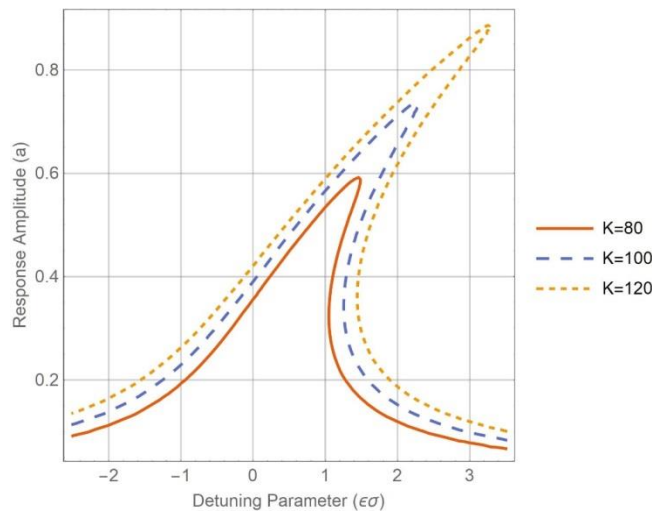


Fig 3. The frequency-response curve of an SSG nanobeam made of Aluminium for different values of excitation amplitude.

The frequency-response curve for three different materials of Aluminum, Gold ,and Nickel is shown in Figure 4 . On can observe that among these three elements, a nanobeam made of Nickel proves to have a higher maximum amplitude and jump height. So it is expected to present higher sensitivity when used in MEMS sensors.

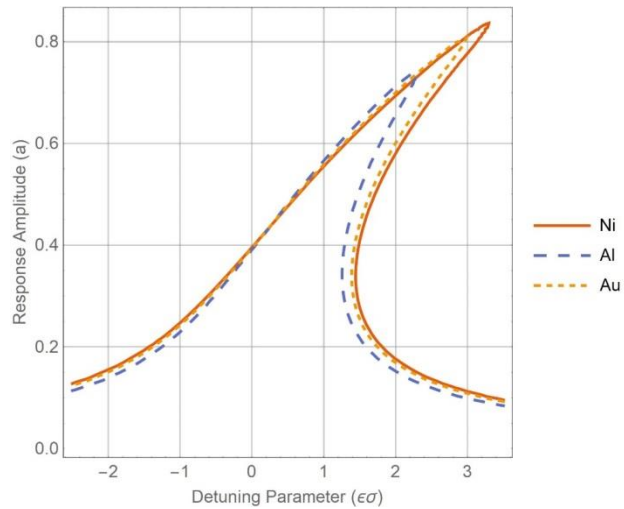


Fig 4. Frequency-response curve for three different materials

The response amplitude vs. the excitation amplitude of three systems made of different materials are presented in Figure 5. It is seen that beams of the same size made of nickel and gold exhibit close behavior in the presence of primary resonance excitation. It is also concluded that the range of the multivalued region is much higher in nickel and gold nanobeams when compared to one made of Aluminum, i.e. for a wider range of excitation amplitudes, one can observe the multivalued response.

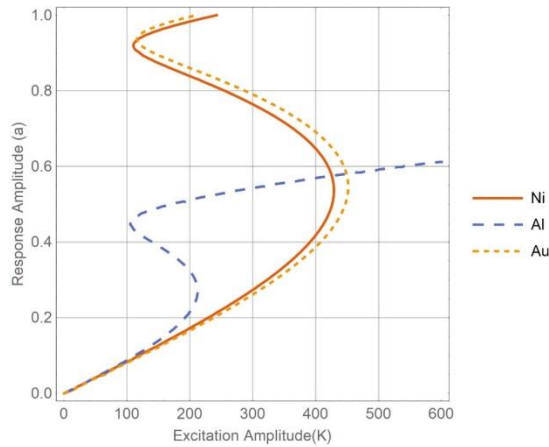


Fig 5. The response vs. excitation amplitude curve for different materials

In Figure 6 the effect of the detuning parameter $\epsilon\sigma$ on the response-excitation amplitude curve is shown. It is understood that there's a critical value of the frequency after which the amplitude of the system is multivalued. It is observed in Figure 6 that increasing the excitation frequency of the nonlinear nanobeam, the deviation of the system response from the linear state also rises and thus, for a wider range of excitation amplitudes, the multivaluedness phenomenon can be witnessed.

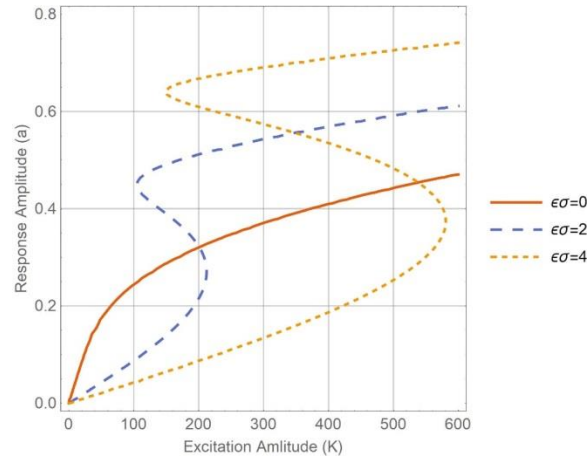


Fig 6. Effect of the detuning parameter on the $a-K_Q$ diagram.

3.1. Comparison with different higher-order theories

Assuming the external load to be zero ($KQ=0$), one can illustrate the ratio of the second strain gradient nonlinear frequency of the nanobeam to the classic linear frequency, versus the ratio of the beam thickness to the lattice parameter as in Figure 7. Setting all b_i 's and c_i 's in the material length scales equal to zero, one can obtain the results based on the (first) strain gradient theory. Furthermore, assuming all the length-scale parameters to be zero will produce the results of the classical beam models. It is seen that the results of the presented paper are in good agreement with the ones obtained by Karparvarfard *et al.* [14]. It is also seen that the size effects are considerable in obtaining the frequency of the nanobeam only when the thickness is small. Figure 7 also predicts higher nonlinear frequency in the second strain gradient theory in comparison to the strain gradient theory which implies that a second strain gradient nanobeam may have a rather stiffer behavior compared to a (first) strain gradient beam.

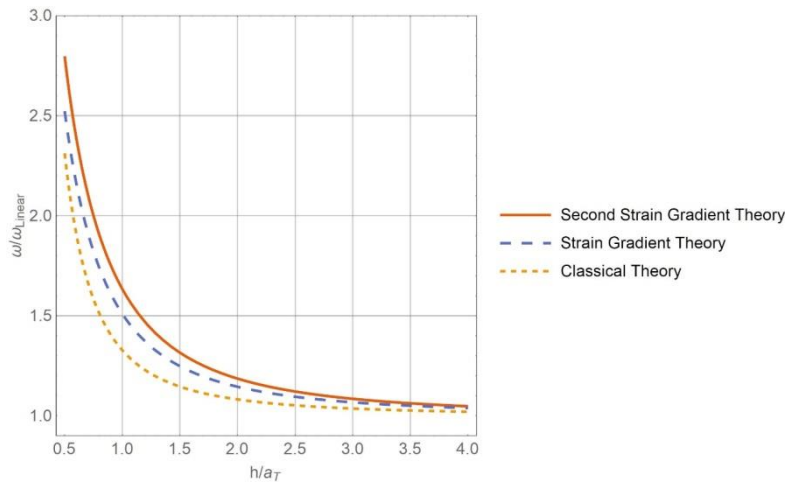


Fig 7. The Frequency ratio of an SSG nanobeam in comparison to SG and classical theories.

4. Conclusion

In this work, the primary resonance of a second strain gradient hinged-hinged Euler-Bernoulli nanobeam is investigated. The second strain gradient theory is a very powerful higher-order

continuum theory capable of taking size effects into account. This theory accounts for surface tension and adds sixteen higher-order material parameters in addition to the Lamé constants. In the framework of the SSG theory, the governing equation of motion has been obtained using Hamilton's principle. Then, after implementing the Galerkin's method, the method of multiple scales has been applied to reach the frequency-response curve for nanobeams made of three different materials. Among these three materials, the Aluminium nanobeam exhibited a stiffer dynamical behaviour and lower maximum amplitude and jump height. It is also shown that the nonlinear vibration of a second strain gradient Euler-Bernoulli nanobeam is size-dependent and that decreasing the thickness not only makes the system stiffer, but also reduces the hardening nonlinearity. The size effects diminish as the thickness of the beam increases. Further, it is shown that increasing the amplitude of the excitation increases the response amplitude and there's a critical value for the excitation frequency of the system after which the response becomes multivalued. The nonlinear frequency of the presented model is then compared to the previously published articles and a good agreement between the SSG theory and the strain gradient theory is observed.

References

- [1] L.J. Currano, M. Yu, B. Balachandran, Latching in a MEMS shock sensor: Modeling and experiments, *Sensors and Actuators A: Physical*, 159 (2010) 41-50.
- [2] L. Li, Z.J. Chew, Microactuators: Design and technology, in: *Smart Sensors and MEMs*, Elsevier, 2018, pp. 305-348.
- [3] Z. Djurić, I. Jokić, A. Peleš, Fluctuations of the number of adsorbed molecules due to adsorption-desorption processes coupled with mass transfer and surface diffusion in bio/chemical MEMS sensors, *Microelectronic Engineering*, 124 (2014) 81-85.
- [4] S. Kong, S. Zhou, Z. Nie, K. Wang, The size-dependent natural frequency of Bernoulli-Euler micro-beams, *International Journal of Engineering Science*, 46 (2008) 427-437.
- [5] W.T. Koiter, Couple-stresses in the theory of elasticity, I and II, *Prec. Roy. Netherlands Acad. Sci. B*, 67 0964.
- [6] R.D. Mindlin, H.F. Tiersten, Effects of couple-stresses in linear elasticity, *Archive for Rational Mechanics and analysis*, 11 (1962) 415-448.
- [7] W. Su, S. Liu, Vibration analysis of periodic cellular solids based on an effective couple-stress continuum model, *International Journal of Solids and Structures*, 51 (2014) 2676-2686.
- [8] F.A.C.M. Yang, A.C.M. Chong, D.C.C. Lam, P. Tong, Couple stress based strain gradient theory for elasticity, *International Journal of Solids and Structures*, 39 (2002) 2731-2743.
- [9] S.K. Park, X.L. Gao, Bernoulli-Euler beam model based on a modified couple stress theory, *Journal of Micromechanics and Microengineering*, 16 (2006) 2355.
- [10] M. Asghari, M.H. Kahrobaiyan, M.T. Ahmadian, A nonlinear Timoshenko beam formulation based on the modified couple stress theory, *International Journal of Engineering Science*, 48 (2010) 1749-1761.
- [11] M. Asghari, M.T. Ahmadian, M.H. Kahrobaiyan, M. Rahaeifard, On the size-dependent behavior of functionally graded micro-beams, *Materials & Design* (1980-2015), 31 (2010) 2324-2329.
- [12] M. Asghari, M. Rahaeifard, M.H. Kahrobaiyan, M.T. Ahmadian, The modified couple stress functionally graded Timoshenko beam formulation, *Materials & Design*, 32 (2011) 1435-1443.
- [13] R.D. Mindlin, Second gradient of strain and surface-tension in linear elasticity, *International Journal of Solids and Structures*, 1 (1965) 417-438.
- [14] S.M.H. Karparvarfar, M. Asghari, R. Vatankhah, A geometrically nonlinear beam model based on the second strain gradient theory, *International Journal of Engineering Science*, 91 (2015) 63-75.
- [15] S.A. Momeni, M. Asghari, The second strain gradient functionally graded beam formulation, *Composite Structures*, 188 (2018) 15-24.
- [16] H. Shodja, F. Ahmadpoor, A. Tehrani, Calculation of the additional constants for fcc materials in second strain gradient elasticity: behavior of a nano-size Bernoulli-Euler beam with surface effects, *Journal of applied mechanics*, 79 (2012).

- [17] R.D. Mindlin, N.N. Eshel, On first strain-gradient theories in linear elasticity, *International Journal of Solids and Structures*, 4 (1968) 109-124.
- [18] R. Ansari, R. Gholami, M.F. Shojaei, V. Mohammadi, S. Sahmani, Size-dependent bending, buckling and free vibration of functionally graded Timoshenko microbeams based on the most general strain gradient theory, *Composite Structures*, 100 (2013) 385-397.
- [19] D.C.C. Lam, F. Yang, A.C.M. Chong, J. Wang, P. Tong, Experiments and theory in strain gradient elasticity, *Journal of the Mechanics and Physics of Solids*, 51 (2003) 1477-1508.
- [20] M.H. Kahrobaiyan, M. Asghari, M. Rahaeifard, M.T. Ahmadian, A nonlinear strain gradient beam formulation, *International Journal of Engineering Science*, 49 (2011) 1256-1267.
- [21] H. Mohammadi, M. Mahzoon, Thermal effects on postbuckling of nonlinear microbeams based on the modified strain gradient theory, *Composite Structures*, 106 (2013) 764-776.
- [22] H. Mohammadi, S. Sepehri, Analyzing dynamical snap-through of a size dependent nonlinear micro-resonator via a semi-analytic method, *Journal of Theoretical and Applied Vibration and Acoustics*, 4 (2018) 19-36.
- [23] F. Amiot, An Euler–Bernoulli second strain gradient beam theory for cantilever sensors, *Philosophical Magazine Letters*, 93 (2013) 204-212.
- [24] S. Khakalo, J. Niiranen, Form II of Mindlin's second strain gradient theory of elasticity with a simplification: For materials and structures from nano-to macro-scales, *European Journal of Mechanics-A/Solids*, 71 (2018) 292-319.
- [25] R.A. Toupin, Elastic materials with couple-stresses, *Archive for Rational Mechanics and Analysis*, 11 (1962) 385-414.
- [26] W. Thomson, *Theory of vibration with applications*, CrC Press, 2018.
- [27] A.H. Nayfeh, D.T. Mook, *Nonlinear oscillations*, John Wiley & Sons, 2008.
- [28] R. Vatankhah, M.H. Kahrobaiyan, A. Alasty, M.T. Ahmadian, Nonlinear forced vibration of strain gradient microbeams, *Applied Mathematical Modelling*, 37 (2013) 8363-8382.